



Universidad Autónoma
de Madrid

Biblos-e Archivo
Repositorio Institucional UAM

Repositorio Institucional de la Universidad Autónoma de Madrid
<https://repositorio.uam.es>

Esta es la **versión de autor** del artículo publicado en:
This is an **author produced version** of a paper published in:

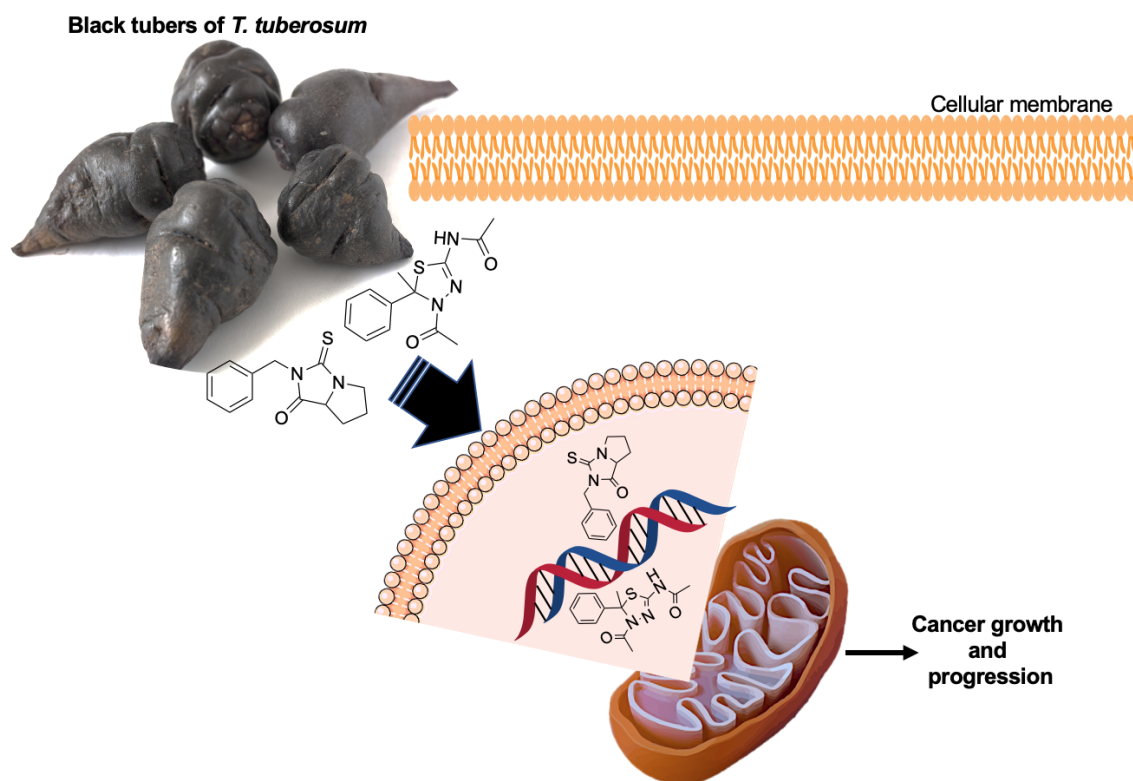
Phytochemistry 177 (2020): 112435

DOI: <https://doi.org/10.1016/j.phytochem.2020.112435>

Copyright: © 2020 Elsevier Ltd. This manuscript version is made available under the CC-BY-NC-ND 4.0 licence <http://creativecommons.org/licenses/by-nc-nd/4.0/>

El acceso a la versión del editor puede requerir la suscripción del recurso
Access to the published version may require subscription

Alkaloids isolated from *Tropaeolum tuberosum* with cytotoxic activity and apoptotic capacity in tumour cell lines



Isolated *T. tuberosum* compounds interact on the DNA chain.

Alkaloids isolated from *Tropaeolum tuberosum* with cytotoxic activity and apoptotic capacity in tumour cell lines

Luis Apaza Ticona^{a,b,*}, Julia Arnanz Sebastián^a, Andreea Madalina Serban^c, Ángel Rumero Sánchez^a

Affiliation

^a*Department of Organic Chemistry, Faculty of Sciences, University Autónoma of Madrid. Cantoblanco, 28049 Madrid, Spain*

^b*Department of Pharmacology, Pharmacognosy and Botany, Faculty of Pharmacy, University Complutense of Madrid. Ciudad Universitaria s/n, 28040 Madrid, Spain*

^c*Maria Sklodowska Curie University Hospital for Children. Constantin Brancoveanu Boulevard, 077120 Bucharest, Romania*

***Corresponding author**

E-mail addresses: luis.apaza@uam.es; lnapaza@ucm.es (Luis Apaza T.).

ABSTRACT

Two alkaloids were isolated and identified for the first time in the black tubers of *Tropaeolum tuberosum*, collected from the Titicani-Taca, Ingavi province in La Paz, Bolivia. Their structures were elucidated by extensive NMR and MS spectroscopic analyses. The isolated compounds were evaluated for their cytotoxicity and apoptotic capacity against four human cancer cell lines. 2-Benzyl-3-thioxohexahydropyrrolo[1,2-c]imidazol-1-one (**1**) showed slight cytotoxic activity against all the cancer cell lines which were tested, with IC₅₀ values ranging from 27.45±0.80 to 31.07±0.87 μM. Moreover, *N*-(4-acetyl-5-methyl-5-

phenyl-4,5-dihydro-1,3,4-thiadiazol-2-yl) acetamide (**2**) showed significant anti-cancer potential, with IC₅₀ values between 1.26±0.57 µM and 1.37±0.09 µM against all human cancer cell lines which were tested. Treatment of tumour cell lines with the compounds caused an increase in the apoptotic rate of these cells, observing that compound **2** presented an apoptotic effect which was double with respect to the control (Dimethylenastron).

Keywords:

Tropaeolum tuberosum, Tropaeolaceae, cytotoxicity, apoptosis, alkaloids.

1. Introduction

Tropaeolum tuberosum Ruiz & Pavón (Tropaeolaceae), a native Andean plant, is traditionally consumed by the indigenous population as food and remedy for various ailments since pre-Columbian times (Fernández & Rodríguez, 2007; Grau et al., 2003). Its tubers have been widely used for the treatment of lung (White, 1975), digestive (Veizaga, 1992), urinary (Espinosa et al., 1994), venereal (Monteros, 1996) and skin (Pérez, 1947) diseases. Several pharmacological studies showed that the tubers of *Tropaeolum tuberosum* have various pharmacological properties, such as antimicrobial (Apaza et al., 2020a), antioxidant (Chirinos et al., 2008), anti-inflammatory (Apaza et al., 2019), anti-spermatogenic (Leiva-Revilla et al., 2012) and benign prostatic anti-hyperplasia (Aire-Artezano et al., 2012). These activities are closely related to its characteristic constituents, such as anthocyanins, macamides glucosinolates and isothiocyanates (Apaza et al., 2020b).

In recent phytochemical investigations, different types of groups of compounds have been isolated from the tubers of this species, such as: phenolic acids, tannins, anthocyanins, glucosinolates, isothiocyanates, phytosterols, fatty acids, macamides and phosphorylated compounds (Apaza et al., 2020b). Our continuous study in this plant led to the isolation and

elucidation of two alkaloids from their respective tubers. The isolation, structural elucidation, cytotoxic activity and apoptotic capacity of these compounds are reported in this document.

2. Results and discussion

The black tubers from *T. tuberosum* were successively extracted with *n*-heptane, CH₂Cl₂/MeOH and water. The CH₂Cl₂/MeOH extract was repeatedly fractionated by column chromatography on silica gel. Two alkaloids were separated and elucidated using various isolation and characterisation techniques (Figure 1).

Figure 1.

2-Benzyl-3-thioxohexahydropyrrolo[1,2-c]imidazol-1-one (**1**) was obtained as a white solid. The HRESIMS data (m/z 247.0720 [M+H]⁺) established a corresponding C₁₃H₁₄N₂OS molecular formula with an unsaturation degree of 8. The ¹³C NMR spectrum confirmed the presence of 4 CH₂ groups, 4 CH groups and 2 quaternary carbon atoms, at δ_C 173.92, which turns out to be a characteristic displacement of tertiary amides, and a displacement of δ_C 187.25, characteristic of substituted thioureas. The ¹H NMR spectrum showed a group of aromatic protons at δ_H 7.28-7.47, a characteristic of a monosubstituted aromatic ring, and two protons of the methylene group at δ_H 5.05 (d, $J=14.5$ Hz) and δ_H 4.96 (d, $J=14.5$ Hz), corresponding to benzyl protons CH₂-1'. At δ_H 4.22, a double-double corresponding to a CH was detected, and at δ_H 4.02 and 3.62, two signals (multiplet) corresponding to a CH₂ group were identified. At high field, two groups of multiples corresponding to two CH₂ groups could be observed (δ_{H-6} 2.29 and 2.18; δ_{H-7} 2.29 and 1.71), with the multiplicity of the signals indicating the presence of a ring (Table 1).

Table 1.

The final assignment of the molecule was carried out by means of the ^1H - ^1H COSY, HSQC and HMBC spectra. In the ^1H - ^1H COSY spectrum, two spin systems were distinguished, from which one corresponds to the benzene system and another one corresponds to the $\text{CH-CH}_2\text{-CH}_2\text{-CH}_2$ system. Positions 8 and 1' have been key factors in this final stage of spectra analysis. Position 8 through HMBC has confirmed the presence of a 5-member cyclic ring in the molecule through a bridge nitrogen (4), which is part of the thiourea bond, as well as the $J_{2,3}$ correlation to H-8 with C-5. In addition, H-8 showed correlation with C-1, corresponding to the carbonyl group of the amide bond (1). The presence of a 5-membered cyclic ring in the molecule was confirmed by the HMBC correlation of 1' with the thiourea group (3) carbonyl and the amide group carbonyl. In addition, the 1' benzyl position led us to the conclusion that it serves as a bridge between the two spin systems (Figure 2). Finally, the determination of the optical rotation of compound **1** gave a value of $[\alpha]^{25}_{\text{D}} -16.5$, indicating that this compound is the “Levogyre enantiomer”.

Regarding the absolute configuration, the compound has an asymmetric carbon atom (C8). In some cases, the *R-S* system proposed by Cahn, Ingold and Prelog can coincide with the denomination Dextrogyre-Levogyre when there is only one asymmetric carbon, where D equal to *R* and L equal to *S*.

In the case of compound **1**, since the optical rotation is Levogyre, we can deduce that it has an *S* configuration, the absolute configuration being (*S*)-(-)-2-Benzyl-3-thioxohexahydropyrrolo [1,2-*c*] imidazol-1-one. This configuration was compared to previously reported references.

Figure 2.

Likewise, there are works that indicate that this compound can be obtained by chemical synthesis, from benzylamine that reacts with 1-(Methyldithiocarbonyl)imidazole in methanol with soft stirring in reflux. Subsequently, the intermediate resulting product is reacted with (*S*)-Methylpyrrolidine-2-carboxylate hydrochloride in triethanolamine and methanol with soft stirring in reflux to obtain compound (*S*)-(-)-2-Benzyl-3-thioxohexahydropyrrolo [1,2-*c*]imidazol-1-one (Sundaram et al., 2007) (Figure 3).

Figure 3.

N-(4-Acetyl-5-methyl-5-phenyl-4,5-dihydro-1,3,4-thiadiazol-2-yl) acetamide (**2**) was obtained as a white powder. The HRESIMS data (m/z 278.0966 $[M+H]^+$ and m/z 300.0785 $[M+Na]^+$) led us to a corresponding $C_{13}H_{15}N_3O_2S$ molecular formula with an unsaturation degree of 8. The ^{13}C NMR spectrum confirmed the presence of 3 CH_3 groups, 5 CH groups and 4 quaternary carbon atoms. The 1H NMR spectrum showed a group of aromatic protons (δ_H 7.26-7.41) characteristic of a monosubstituted benzene ring. The signals of the CH groups in the phenyl substituent were assigned according to the multiplicity and correlations in 1H - 1H COSY, HMBC and HSQC spectra (Table 2).

Table 2.

The equivalent protons H-2' and H-6' (δ_H 7.41, $J=7.5$ Hz) were coupled with the protons H-3' and H-5' (δ_H 7.34, $J=7.5$ Hz), respectively, and over long distance with the proton H-4' (δ_H 7.26, $J=1.5$ Hz). HMBC spectrum was used to locate the closest carbon in the thiadiazolic ring C5 (δ_C 80.92), showing 3J HMBC correlation with the protons H-2' and H-6'. The other quaternary carbon atom C-2 (δ_C 145.10) in the thiadiazolic ring showed 4J

HMBC correlation with the methyl group CH₃-9 (δ_{H} 2.08, δ_{C} 22.57), which showed 2J HMBC correlation with C-8 (δ_{C} 171.52). In addition, the methyl group CH₃-6 (δ_{H} 2.34, δ_{C} 27.14) was assigned by 2J HMBC correlation with C-5 and 3J HMBC correlation with C-1' (δ_{C} 144.70). Finally, the remaining methyl group CH₃-11 was assigned at δ_{H} 2.25 and δ_{C} 23.78, which showed 2J HMBC correlation with C-10 (δ_{C} 171.16) (Figure 4). Finally, the determination of the optical activity of compound **2** gave a value of zero, which indicates that this compound is optically inactive because it is a mixture of its 2 enantiomers, caused by the asymmetric carbon (C5).

In this case, any possible orientation of one enantiomer is counteracted by the presence of the other enantiomer, cancelling all possible rotations. This equimolar mixture of the (*R*) and (*S*) enantiomers is called racemic modification and does not show rotation of the plane of polarised light, so our compound is (\pm)-*N*-(4-acetyl-5-methyl-5-phenyl-4,5-dihydro-1,3,4-thiadiazol-2-yl) acetamide. This configuration was compared with previously reported references.

Figure 4.

Previous research indicates that this compound is obtained by chemical synthesis, from acetophenone that reacts with thiosemicarbazide in methanol with vigorous stirring to provide (*E*)-2-(1-phenylethylidene)hydrazine-1-carbothioamide. Subsequently, this intermediate compound undergoes a cyclisation and a subsequent acetylation reaction in acetic anhydride to obtain compound (\pm)-*N*-(4-acetyl-5-methyl-5-phenyl-4,5-dihydro-1,3,4-thiadiazol-2-yl) acetamide (Yamamoto et al., 2014; Murakata et al., 2007) (Figure 5).

Figure 5.

The phytochemical study carried out on the tubers of *T. tuberosum* led to the isolation of alkaloids derived from thiohydantoin and 1,3,4-thiadiazoline, which are groups of specialised metabolites found in hypocotyls of Maca (*Lepidium meyenii* Walp). This class of compounds has been considered as characteristic biomarkers of Maca (Huang et al., 2018), however, this study shows us that there is a connection between these two Andean species. This statement can be supported by the fact that both species grow in countries that are found in the Andes. In this region these species are exposed to extreme climatic conditions such as poor soils with a slightly acidic pH between 5-6 and exposures to ultraviolet radiation at altitudes of 3.800 meters above sea level, producing similar specialised metabolites (Apaza et al., 2020b; Carvalho & Ribeiro, 2019).

Due to the culture conditions mentioned above, the alkaloids (specialised metabolites) present in this species can be formed from the degradation of glucosinolates by the enzyme myrosinase resulting in the formation of isothiocyanates (Sánchez-Pujante et al., 2017). Subsequently, the resulting isothiocyanates can react with amino acids (proline) or with compounds derived from weak acids (acetamide) through a combination of the Edman degradation and Aldol condensation reactions (Huang et al., 2018) (Figure 6).

Figure 6.

This class of alkaloids are very unusual because they have a basic nucleus consisting of nitrogen and sulphur, which gives it a particularly high density of interaction sites for polar interactions and hydrogen bonds. Furthermore, these alkaloids can present optical isomerism, with relevance in pharmacomodulation, due to the specificity of biological targets towards a specific enantiomer or towards the combination of both enantiomers (Motaïs de Narbonne et al., 2016; Nguyen et al., 2006; McConathy & Owens, 2003). Therefore, these compounds can

have a variety of applications, such as anti-inflammatory, anti-ulcer, apoptosis induction, induction and inhibition of gene expression (Debnath et al., 2018).

The cytotoxic activity of compounds **1** and **2** was evaluated against four human cancer cell lines: A549 (lung cancer), Caki-1 (renal cancer), T24 (urinary bladder cancer) and PC-3 (prostatic cancer) (Table 3). Both showed cytotoxic activity in all human cancer cell lines compared to the positive control, Dimethylenastron ($CC_{50}=0.23 \mu M$). Compound **1**, a thiohydantoin-derived alkaloid, showed slight cytotoxic activity in all human cancer cell lines, with CC_{50} values ranging from 27.45 ± 0.80 to $31.07\pm0.87 \mu M$. It also showed increased cytotoxicity in the human urinary bladder carcinoma (T24) cell line. Concerning compound **2**, an alkaloid derived from 1,3,4-thiadiazoline, it showed significant cytotoxic activity in all human cancer cell lines, with CC_{50} values ranging from 1.26 ± 0.57 to $1.37\pm0.09 \mu M$, and increased cytotoxicity in the human prostate carcinoma (PC-3) cell line.

Table 3.

To study the nature of compounds-induced cell death, cells were treated and then analysed by flow cytometry using a combination of Rhodamine 123 and PI staining as an apoptotic/necrotic cell marker. Figure 7 shows the results of Rho123/PI staining in different tumour cell lines after exposure for 72 h to the compounds and to the positive control (Dimethylenastron) at an $IC_{50}=0.23 \mu M$. The data demonstrated a significant increase in the percentage of apoptosis of the isolated *T. tuberosum* compounds in all cell lines after treatment. Compound **1** behaved in the same way as the positive control by promoting apoptosis of the different tumour cell lines at an IC_{50} of $29.06 \mu M$. However, compound **2** increased apoptosis of A549 (20.03%); Caki-1 (25.80%); T24 (21.68%) and PC-3 (23.97%) cell lines treated at an IC_{50} of $1.33 \mu M$ for 72 h compared to untreated cells. Likewise, the

induction of apoptosis by compound **2** was greater than that caused by the positive control (Dimethylenastron), an inhibitor of the mitotic motor kinesin Eg5. This assay allowed us to establish that the compounds act by the apoptotic pathway dependent on intrinsic mitochondria, considering that rhodamine 123 is related to alterations in mitochondrial transmembrane potential.

Figure 7.

Concerning compound **1**, there are reports in the literature on compounds derived from thiohydantoin showing anticancer activity against human cervical carcinoma (HeLa) and breast carcinoma cell lines (MCF-7) by inhibiting Top1 (Majumdar et al., 2015). Top1 (Topoisomerase 1) is an essential enzyme that induces transient single-strand breaks at different sites in the genome, generating Top1-DNA cleavage complexes. Under normal conditions these complexes are highly transient, however they can be stabilised by compounds that specifically bind at the Top1-DNA interface. These stabilised complexes can cause DNA damage, initiating cellular responses that include apoptosis (Wang, 2002). In our case, due to the similarity of the chemical structure with those reported in later works and the results obtained from cytotoxicity and apoptotic capacity tests, we can indicate that compound **1** has the same mechanism of action.

Concerning compound **2**, an alkaloid derived from 1,3,4-thiadiazoline, previous reports have demonstrated the antitumor activity of this compound as a **racemic mixture**, against different tumour cell lines, such as: glioblastoma U-87 MG and U-251 MG (Taglieri et al., 2018); melanoma SK-MEL-5 and SK-MEL-28 (Giantulli et al., 2018; De monte et al., 2015); breast cancer MCF7, BT474, SKBR3 and MDA-MB231 (De Iuliis et al., 2016); colorectal carcinoma HCT116 (Nakai et al., 2009). The mechanism of action of the **racemic mixture**

(compound **2**) reported in each of the works mentioned above is the specific inhibition of microtubules-stimulated Eg5 ATPase activity in an ATP-uncompetitive manner, inducing in the monoastal spindles, subsequently causing a mitotic arrest and finally an apoptosis in the tumour cells.

Mitotic kinesins (Eg5) are important regulators of the response and migration of cancer cells, since these proteins play an important role in the formation of the bipolar mitotic spindle and in the regulation of cell cycle progression in many tumours. Its inhibition can lead to spindle assembly checkpoint mediated cell cycle arrest in mitosis, causing cell death due to apoptosis, necrosis or autophagy (Rath & Kozielski, 2012). According to the reported literature and to our data on the cytotoxicity and apoptotic capacity of compound **2**, we can corroborate that it presents antitumor activity.

Currently, compounds that act on the mitotic spindle are under investigation among cancer therapies and they are considered to be more effective (Jordan and Wilson, 2004). In this sense, the antitumor capacity of the isolated compounds of *T. tuberosum* tubers would be of great interest in this area, given that they act on two sites of action, Eg5 in the case of compound **2** and Top 1 in the case of compound **1**. Moreover, a series of analogues can be developed starting from the compounds reported in the current article allowing thus the maximisation of their action on the Top1 and Eg5 targets.

3. Material and methods

3.1. General experimental procedures

1D and 2D NMR spectra were recorded on 250 MHz Bruker Analytische Messtechnik GmbH spectrometer operated at 250 MHz (¹H) or 60 MHz (¹³C) and Bruker BioSpin GmbH operated at 700 MHz (¹H) or 176 MHz (¹³C), with TMS as the internal standard. The

deuterated solvents were CDCl_3-d_1 ; $\text{MeOD}-d_4$ and D_2O . Spectra were calibrated by assignment of the residual solvent peak to δ_{H} 7.26; δ_{H} 3.31 and δ_{H} 4.79 for CDCl_3 , MeOD and D_2O , and δ_{C} 77.16 and δ_{C} 49.00, for CDCl_3 and MeOD . The complete assignment of protons and carbons was done by analysing the correlated ^1H - ^1H -COSY, HSQC and HMBC spectra. Mass spectra were performed on a mass spectrometer with a QTOF hybrid model QSTAR *pulsar i analyser* from the commercial company AB Sciex. The samples were analysed using the electrospray ionisation technique in positive ion detection mode. They were introduced into the mass spectrometer by direct infusion at a flow of $10\ \mu\text{L}/\text{min}$, using a syringe pump. Column chromatography was performed with silica gel (20-45 μm and 40-63 μm , Merck). TLC was performed using silica gel 60-F₂₅₄ plates (Merck). Fractions were monitored by TLC, spots were visualised by UV absorbance (254 nm), and the silica gel plates were subsequently sprayed with phosphomolybdic acid and finally heated.

3.2. Plant material

The tubers of *Tropaeolum tuberosum* Ruiz & Pavón (Tropaeolaceae) were collected from in Titicani-Taca which is located in Villa Asunción de Machaca canton of the Sixth Municipal Section, Jesus de Machaca, in the Ingavi province of La Paz department, Bolivia ($16^\circ 44' 24.5''\ \text{S}$ $68^\circ 48' 49.2''\ \text{W}$), in September 2015, at an altitude of 3900 m. Botanical identification was confirmed by the National Herbarium of Bolivia (No. 14898).

3.3. Extraction and isolation

After air-drying and powdering tubers of *T. tuberosum* (500 g), they were repeatedly extracted with *n*-heptane (3x1 L), $\text{CH}_2\text{Cl}_2/\text{MeOH}$ (3x1 L) and distilled water (3x1 L) at room temperature for 3 days. The solvents were evaporated in vacuum to produce the crude *n*-heptane (71.54 g), $\text{CH}_2\text{Cl}_2/\text{MeOH}$ (26.61 g) and aqueous (125.41 g) extracts. The crude

extract of CH₂Cl₂/MeOH (25 g) was fractionated by silica gel (40-63 μ m) column (2x50 cm) chromatography guided by bioassay, using a gradual gradient of *n*-heptane/AcOEt (30:1→1:1 v/v), obtaining 7 fractions (I→VII), where fraction **V** (4.56 g) showed greater cytotoxic activity and apoptotic capacity in all tumour cell lines. Subsequently, fraction **V** was separated by silica gel (40-63 μ m) column (2x50 cm) chromatography (CH₂Cl₂/acetone, 15:1→1:0 v/v), obtaining 4 sub-fractions (VA→VD) that showed cytotoxic activity and apoptotic capacity in all the tested tumour cell lines, where sub-fraction **VB** (750 mg) had more activity. Subsequently, sub-fraction **VB** was separated by silica gel (20-45 μ m) column (2x50 cm) chromatography (*n*-heptane/acetone, 7:2→1:0 v/v), obtaining 6 subfractions (VB1→VB6), where the subfractions **VB1**-compound **1** (13 mg) and **VB2**-compound **2** (37 mg) showed cytotoxic activity and apoptotic capacity.

3.4. Spectroscopic data

(*S*)-(-)-2-Benzyl-3-thioxohexahydropyrrolo[1,2-*c*]imidazol-1-one (**1**), white solid; [α]_D²⁵ -16.5 (*c* 0.1, CHCl₃); IR (KBr) ν_{\max} 3057, 2973, 2930, 1743, 1459, 1348, 1245, 1260, 1220, 1165, 963 cm⁻¹; ¹H and ¹³C NMR data, see Table 1; HRESIMS *m/z* 247.0720 [M+H]⁺ (calcd for C₁₃H₁₅N₂OS, 247.0905).

(±)-*N*-(4-Acetyl-5-methyl-5-phenyl-4,5-dihydro-1,3,4-thiadiazol-2-yl) acetamide (**2**), white powder; [α]_D²⁵ 0 (*c* 0.1, CH₃OH); IR (KBr) ν_{\max} 3147, 1695, 1630, 1610 cm⁻¹; ¹H and ¹³C NMR data, see Table 2; HRESIMS *m/z* 278.0966 [M+H]⁺ and 300.0785 [M+Na]⁺ (calcd for C₁₃H₁₆N₃O₂S, 278.0963 and C₁₃H₁₅N₃O₂SNa, 300.0783).

3.5. Cell culture

Four human cancer cell lines were used in this study: A549 (Human lung carcinoma, CCL-185), Caki-1 (Human renal carcinoma, HTB-46), T24 (Human urinary bladder

carcinoma, HTB-4) and PC-3 (Human prostatic carcinoma, CRL-1435) cancer cell lines. All cell lines were obtained from the ATCC (American Type Culture Collection, Manassas, USA). Cells were cultured in DMEM (Sigma-Aldrich, St. Louis, USA) supplemented with L-glutamine (PanReac AppliChem, Barcelona, Spain), 10% FBS (Fetal bovine serum. Summit Biotechnology; Ft. Collins, CO), 100 U/mL penicillin and 100 μ g/mL streptomycin (Fisher Scientific, Pittsburgh, USA).

3.6. Cell viability assay - XTT

The cells were seeded in 96-well plates (200 μ L, 2×10^4 cells/well) and were grown for 12 h at 37°C in hypoxic conditions (1% O₂), thus mimicking the *in vivo* tumour microenvironment. Subsequently, the cells were treated with the compounds at different concentrations (100 μ M, 50 μ M, 25 μ M, 12.50 μ M, 6.25 μ M, 3.13 μ M, 1.56 μ M, 0.78 μ M, 0.39 μ M and 0.20 μ M) and 200 μ L H₂O₂ (0.1 mM). As a next step, they were cultivated for 72 h. After the treatment, the medium in each well was substituted by 200 μ L of fresh medium, followed by the addition of 50 μ L XTT (0.6 mg/mL) containing 25 μ M PMS. The plate was further incubated for 4 h in the same conditions, and the absorbance was measured at a wavelength of 450 nm in a spectrophotometric ELISA plate reader (SpectraMax® i3, Molecular Devices, CA, USA).

3.7. Apoptosis

Apoptosis was determined by the rhodamine method. A double staining was used (rhodamine 123 to detect changes in the mitochondrial membrane and propidium iodide to detect necrotic cells). The cells (20×10^4) were seeded in 55 mm plates with 2 mL of complete DMEM and treated with the compounds at a concentration obtained by the viability assay XTT (CC₅₀). 72 hours after treatment, cells were incubated with 5 μ L of rhodamine

123 (1 $\mu\text{g}/\mu\text{L}$) for 30 minutes. All cells in each well were harvested and centrifuged at 500 g for 10 minutes. The cell pellet was washed 3 times with 1 mL of PBS 1x + 1% BSA solution and resuspended in 500 mL of PBS 1x + 1% BSA solution containing 0.5 mL of propidium iodide (PI) (5 $\mu\text{g}/\mu\text{L}$). The entire procedure was performed at 4°C. The samples were analysed by flow cytometry on the BD-FACSCalibur™ cytometer (Becton Dickinson BioScience, San Jose, CA, USA). Expo32 software was used to analyse the data. The percentage of Rho-negative and PI-negative cells corresponded to the apoptotic population.

3.8. Statistical analysis

All results and data were confirmed in at least three separate experiments. Data are expressed as means \pm SD. Statistical comparisons were analysed by one-way ANOVA followed by Tukey's post hoc test for multiple comparisons using GraphPad Prism software, version 8.2.1 (GraphPad Software Inc., San Diego, CA, USA). $P < 0.0001$ was considered statistically significant.

Conflicts of interest

The authors declare no conflict of interest.

Acknowledgments

This work was supported by the Fundación de la Universidad Autónoma de Madrid (FUAM).

Author contribution

ARS and JAS contributed to the analysis of the spectral data; LAT and AMS contributed to the conception and experimental design of the pharmacological study and LAT contributed to the writing and review of the manuscript.

References

- 352 Aire-Artezano, G., Charaja-Vildoso, R., De la Cruz-Santiago, H., Guillermo-Sánchez, B.,
- 353 Gutarra-Vela, M., Huamaní-Charagua, P., Chilquillo, G.J., Nicho-Póvez, M., Ochoa-
- 354 Gago, M., Pari-Naña, R., 2012. Efecto de *Tropaeolum tuberosum* frente a la hiperplasia
- 355 prostática benigna inducida en ratas holtzman. CIMEL. 18, 1-13.
- 356 <https://doi.org/10.23961/cimel.2013.181.387>
- 357 Apaza T.L., Tena, P.V., Serban A.M., Alonso N.M.J., Rumero A., 2019. Alkamides from
- 358 *Tropaeolum tuberosum* inhibit inflammatory response induced by TNF- α and NF- κ B. J.
- 359 Ethnopharmacol. 235, 199-205. <https://doi.org/10.1016/j.jep.2019.02.015>.
- 360 Apaza, T.L., Rumero, S.A., Orozco, G.O., Ortega, D.M., 2020a. Antimicrobial compounds
- 361 isolated from *Tropaeolum tuberosum*. Natural Product Research.
- 362 <https://doi.org/10.1080/14786419.2019.1710700>.
- 363 Apaza, T.L., Tena, V.P., Bermejo, P.B., 2020b. Local/traditional uses, secondary metabolites
- 364 and biological activities of Mashua (*Tropaeolum tuberosum* Ruíz & Pavón). J.
- 365 Ethnopharmacol. 247, 112152. <https://doi.org/10.1016/j.jep.2019.112152>.
- 366 Carvalho, F.V., Ribeiro, P.R., 2019. Structural diversity, biosynthetic aspects, and LC-HRMS
- 367 data compilation for the identification of bioactive compounds of *Lepidium meyenii*. Food
- 368 Res Int. 125, 108615. <https://doi.org/10.1016/j.foodres.2019.108615>.
- 369 Chirinos, R., Campos, D., Costa, N., Arbizu, C., Pedreschi, R., Larondelle, Y., 2008.
- 370 Phenolic profiles of Andean Mashua (*Tropaeolum tuberosum* Ruíz & Pavón) tubers:
- 371 Identification by HPLC-DAD and evaluation of their antioxidant activity. Food Chem.
- 372 106, 1285-1298. <https://doi.org/10.1016/j.foodchem.2007.07.024>.
- 373 Debnath, B., Singh, W.S., Das, M., Goswami, S., Singh, M.K., Maiti, D., Manna, K., 2018.
- 374 Role of plant alkaloids on human health: A review of biological activities. Material Today
- 375 Chemistry. 9, 56-72. <https://doi.org/10.1016/j.mtchem.2018.05.001>.

- 376 De Iuliis, F., Taglieri, L., Salerno, G., Giuffrida, A., Milana, B., Giantulli, S., Carradori, S.,
377 Silvestri, I., Scarpa, S., 2016. The kinesin Eg5 inhibitor K858 induces apoptosis but also
378 survivin-related chemoresistance in breast cancer cells. *Invest New Drugs*. 34, 399-406.
379 <https://doi.org/10.1007/s10637-016-0345-8>.
- 380 De Monte, C., Carradori, S., Secci, D., D'Ascenzio, M., Guglielmi, P., Mollica, A., Morrone,
381 S., Scarpa, S., Aglianò, A.M., Giantulli, S., Silvestri, I., 2015. Synthesis and
382 pharmacological screening of a large library of 1,3,4-thiadiazolines as innovative
383 therapeutic tools for the treatment of prostate cancer and melanoma. *Eur. J. Med. Chem.*
384 105, 245-262. <https://doi.org/10.1016/j.ejmech.2015.10.023>.
- 385 Espinosa, P., Abad, J., Vaca, R., 1994. Diagnóstico de las limitantes de producción y
386 consumo de las raíces y tubérculos andinos en Ecuador. Instituto Nacional de
387 Investigaciones Agropecuarias (INIAP), pp. irr.
- 388 Fernández, H.A.M., Rodríguez, R.E.F., 2007. Etnobotánica del Perú Pre-Hispano. Ediciones
389 Herbarium Truxillense (HUT). Trujillo, Peru, pp. 133-134.
- 390 Giantulli, S., De Iuliis, F., Taglieri, L., Carradori, S., Menichelli, G., Morrone, S., Scarpa, S.,
391 Silvestri, I., 2018. Growth arrest and apoptosis induced by kinesin Eg5 inhibitor K858 and
392 by its 1,3,4-thiadiazoline analogue in tumor cells. *Anticancer Drugs*. 29, 674-681.
393 <https://doi.org/10.1097/CAD.0000000000000641>.
- 394 Grau, A., Ortega, D.R., Nieto, C.C., Hermann, M., 2003. Mashua *Tropaeolum tuberosum*
395 Ruíz & Pavón. Engels Jan M.M. Rome, Italy, pp. 1-27.
- 396 Huang, Y.J., Peng, X.R., Qiu, M.H., 2018. Progress on the Chemical Constituents Derived
397 from Glucosinolates in Maca (*Lepidium meyenii*). *Nat. Prod. Bioprospect*. 8, 405-412.
398 <https://doi.org/10.1007/s13659-018-0185-7>.
- 399 Jordan, M.A., Wilson, L., 2004. Microtubules as a target for anticancer drugs. *Nat Rev*
400 *Cancer*. 4, 253-265. <https://doi.org/10.1038/nrc1317>.

- 401 Leiva-Revilla, J., Cárdenas-Valencia, I., Rubio, J., Guerra-Castañón, F., Olcese-Mori, P.,
 402 Gasco, M., Gonzales, G.F., 2012. Evaluation of different doses of Mashua (*Tropaeolum*
 403 *tuberosum*) on the reduction of sperm production, motility and morphology in adult male
 404 rats. *Andrologia*. 44, 205-212. <https://doi.org/10.1111/j.1439-0272.2011.01165.x>.
- 405 Majumdar, P., Bathula, C., Basu, S.M., Das, S.K., Agarwal, R., Hati, S., Singh, A., Sen, S.,
 406 Das, B.B., 2015. Design, synthesis and evaluation of thiohydantoin derivatives as potent
 407 topoisomerase I (Top1) inhibitors with anticancer activity. *Eur. J. Med. Chem.* 102, 540-
 408 551. <https://doi.org/10.1016/j.ejmech.2015.08.032>.
- 409 McConathy, J., Owens, M.J., 2003. Stereochemistry in Drug Action. *Prim. Care Companion*
 410 *J. Clin. Psychiatry*. 5, 70-73. <https://doi.org/10.4088/pcc.v05n0202>.
- 411 Motaïs de Narbonne, M., van Zweden, J.S., Bello, J.E., Wenseleers, T., Millar, J.G.,
 412 d'Ettorre, P., 2016. Biological Activity of the Enantiomers of 3-methylhentriacontane, a
 413 Queen Pheromone of the Ant *Lasius Niger*. *J. Exp. Biol.* 219, 1632-1638.
 414 <https://doi.org/10.1242/jeb.136069>.
- 415 Monteros Altamirano, A.R., 1996. Estudio de la Variación Morfológica e Isoenzimática de
 416 78 entradas de Mashua (*Tropaeolum tuberosum* R & P.). “Santa Catalina”-INIAP (Ing
 417 Thesis). Facultad de Ciencias Agrícolas. Universidad Central de Ecuador, EC.
- 418 Murakata, C., Ino, Y., Kato, K., Yamamoto, J., Kitamura, Y., Nakai, R., Nakano, T., Tsujita,
 419 T., 2007. Thiadiazoline derivative, US Patent No. 20070276017.
- 420 Nakai, R., Iida, S-I., Takahashi, T., Tsujita, T., Okamoto, S., Takada, C., Akasaka, K.,
 421 Ichikawa, S., Ishida, H., Kusaka, H., Akinaga, S., Murakata, C., Honda, S., Nitta, M.,
 422 Saya, H., Yamashita, Y., 2009. K858, a Novel Inhibitor of Mitotic Kinesin Eg5 and
 423 Antitumor Agent, Induces Cell Death in Cancer Cells. *Cancer Res.* 69, 3901-3909.
 424 <https://doi.org/10.1158/0008-5472.CAN-08-4373>.

- 425 Nguyen, L.A., He, H., Pham-Huy, C., 2006. Chiral drugs: an overview. *Int. J. Biomed. Sci.* 2,
426 85-100.
- 427 Pérez, A.E., 1947. *Plantas útiles de Colombia. Ensayo de botánica colombiana aplicada.*
428 Imprenta Nacional. Bogota, Colombia.
- 429 Rath, O., Kozielski, F., 2012. Kinesins and cancer. *Nat. Rev. Cancer.* 12, 527-539.
430 <https://doi.org/10.1038/nrc3310>.
- 431 Sánchez-Pujante, P.J., Borja-Martínez, M., Pedreño, M.A., Almagro, L., 2017. Biosynthesis
432 and Bioactivity of Glucosinolates and Their Production in Plant in Vitro Cultures. *Planta.*
433 246, 19-32. <https://doi.org/10.1007/s00425-017-2705-9>.
- 434 Sundaram, S.G.M., Venkatesh, C., Ila, H., Junjappa, H., 2007. 1-(Methyldithiocarbonyl)
435 imidazole as Thiocarbonyl Transfer Reagent: A Facile One-Pot Three-Component
436 Synthesis of 3,5- and 1,3,5-Substituted- 2-Thiohydantoins. *Synlett.* 2, 0251-0254.
437 <https://doi.org/10.1055/s-2007-967987>.
- 438 Taglieri, L., Rubinacci, G., Giuffrida, A., Carradori, S., Scarpa, S., 2018. The kinesin Eg5
439 inhibitor K858 induces apoptosis and reverses the malignant invasive phenotype in human
440 glioblastoma cells. *Invest New Drugs.* 36, 28-35. [https://doi.org/10.1007/s10637-017-](https://doi.org/10.1007/s10637-017-0517-1)
441 [0517-1](https://doi.org/10.1007/s10637-017-0517-1).
- 442 Veizaga, E., 1992. Diagnóstico de la producción tradicional de tubérculos andinos y su uso
443 en tres comunidades de la provincia Tapacaré. In: *Congreso Internacional sobre Cultivos*
444 *Andinos.* CIID. La Paz-Bolivia, pp. 271-275.
- 445 Wang, J.C., 2002. Cellular roles of DNA topoisomerases: a molecular perspective. *Nat Rev*
446 *Mol Cell Biol.* 3, 430-440. <https://doi.org/10.1038/nrm831>.
- 447 Yamamoto, J., Amishiro, N., Kato, K., Ohta, Y., Ino, Y., Araki, M., Tsujita, T., Okamoto, S.,
448 Takahashi, T., Kusaka, H., Akinaga, S., Yamashita, Y., Nakai, R., Murakata, C., 2014.
449 Synthetic Studies on Mitotic Kinesin Eg5 Inhibitors: Synthesis and Structure-Activity

1081
1082
1083
1084
1085
1086
1087
1088
1089
1090
1091
1092
1093
1094
1095
1096
1097
1098
1099
1100
1101
1102
1103
1104
1105
1106
1107
1108
1109
1110
1111
1112
1113
1114
1115
1116
1117
1118
1119
1120
1121
1122
1123
1124
1125
1126
1127
1128
1129
1130
1131
1132
1133
1134
1135
1136
1137
1138
1139
1140

450 Relationships of Novel 2,4,5-substituted-1,3,4-thiadiazoline Derivatives. Bioorg. Med.
451 Chem. Lett. 24, 3961-3963. <https://doi.org/10.1016/j.bmcl.2014.06.034>.
452

Legends for Figures

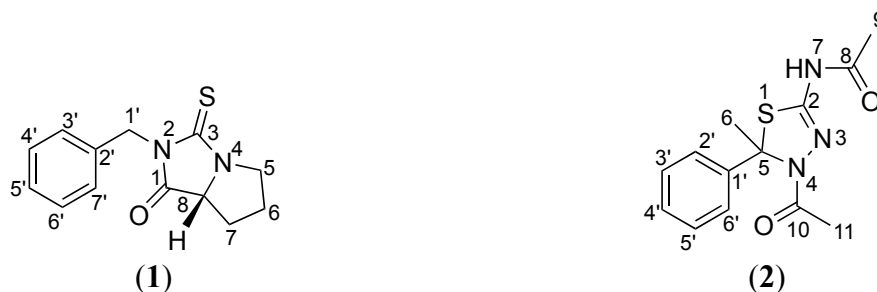


Fig. 1. Chemical structures of compounds **1** and **2** of black tubers from *T. tuberosum*

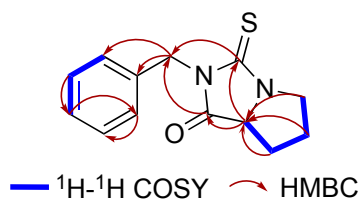


Fig. 2. ^1H - ^1H COSY and HMBC type correlations of compound **1**.

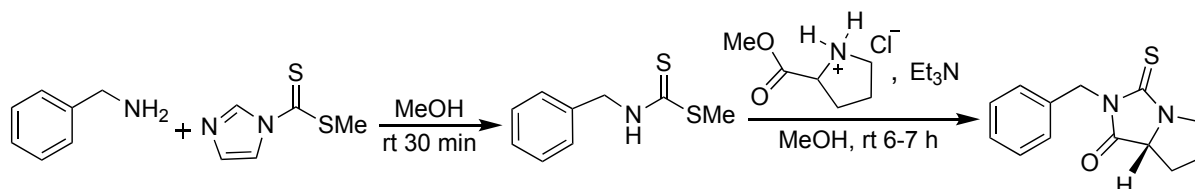


Fig.3. Synthesis of compound **1**.

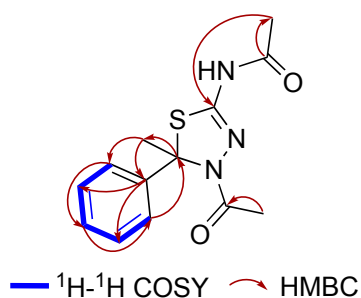


Fig. 4. ^1H - ^1H COSY and HMBC type correlations of compound **2**.

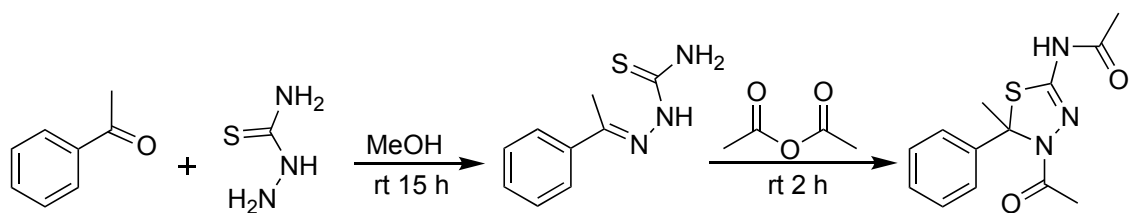


Fig 5. Synthesis of compound **2**.

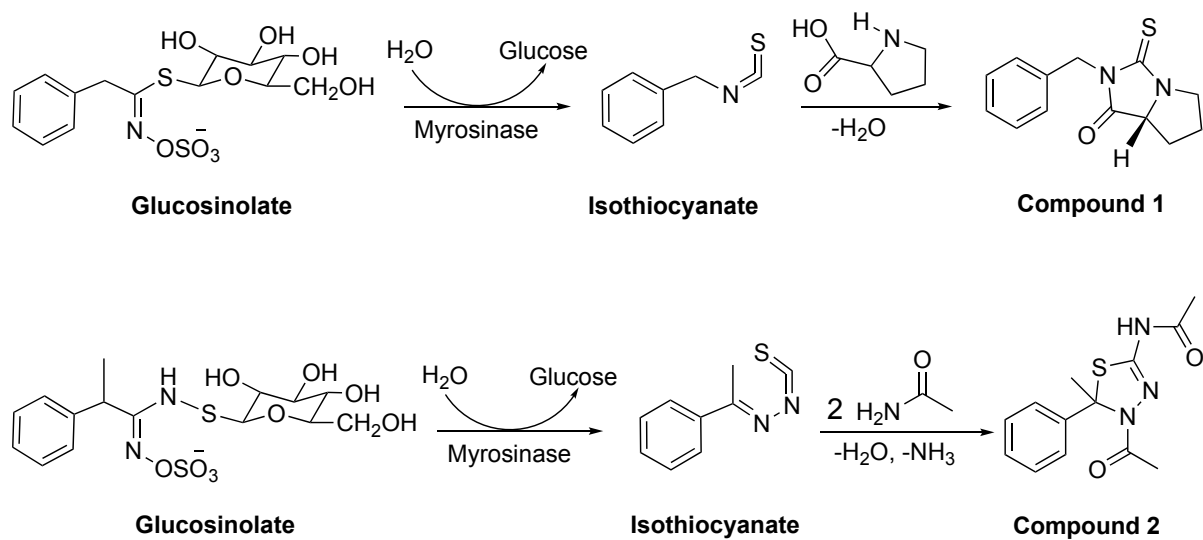
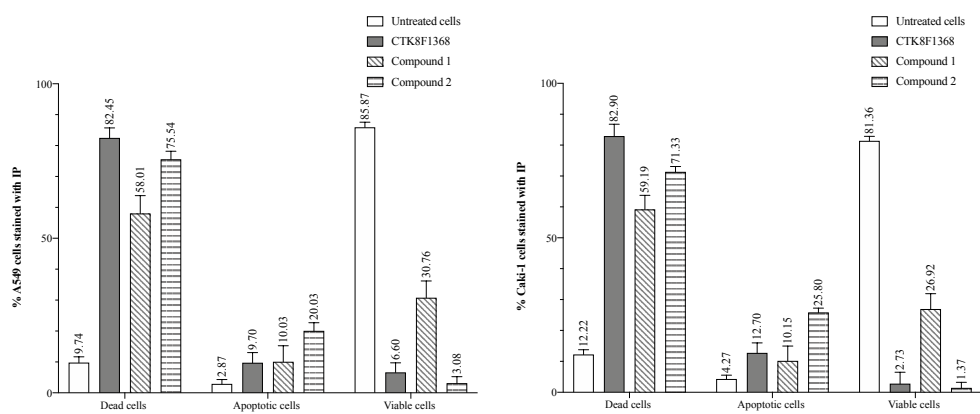


Fig. 6. Biosynthesis of compounds **1** and **2**.



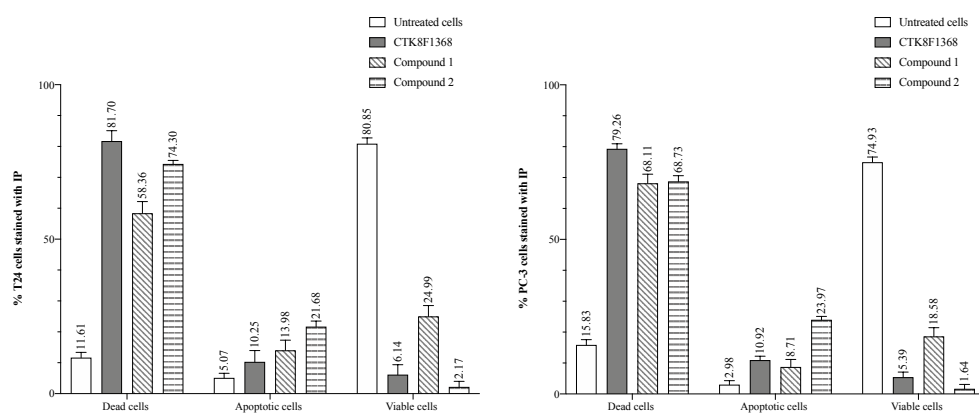


Fig. 7. Effects of compounds on the apoptosis of different tumoral cells. Untreated cells as negative reference, with Dimethylenastron (CTK8F1368), as positive reference compound at $IC_{50}=0.23 \mu M$, with compound 1 at $IC_{50}=29.06 \mu M$ and compound 2 at $IC_{50}=1.33 \mu M$, for 72 h and were stained with fluorochromes Rho123 (Rhodamine 123) and IP (Propidium Iodide) and evaluated by flow cytometry. $p<0.0001$ (t Tukey, Two-way ANOVA).

Legends for Tables

Table 1. ^1H (250 MHz) and ^{13}C (60 MHz) data of compound **1** in CDCl_3-d_1 (δ in ppm).

No.	1	
	δ_{H} , mult. (J in Hz)	δ_{C}
1	-----	173.92
3	-----	187.25
5	4.02 (1H, m, H-5)	48.86
	3.62 (1H, m, H-5)	
6	2.29 (1H, m, H-6)	27.24
	2.18 (1H, m, H-6)	
7	2.29 (1H, m, H-7)	27.20
	1.71 (1H, m, H-7)	
8	4.22 (1H, dd, $J=10.3$; 7.1 Hz)	65.48
1'	5.05 (1H, d, $J=14.6$ Hz, H-1')	45.48
	4.96 (1H, d, $J=14.6$ Hz, H-1')	
2'	-----	136.23
3'	7.47 (1H, d, $J=7.3$ Hz)	129.09
4'	7.32 (1H, dd, $J=7.1$; 7.3 Hz)	128.92
5'	7.28 (1H, t, $J=7.1$ Hz)	128.26
6'	7.32 (1H, dd, $J=7.1$; 7.3 Hz)	128.92
7'	7.47 (1H, d, $J=7.3$ Hz)	129.09

Table 2. ^1H (700 MHz) and ^{13}C (176 MHz) data of compound **2** in $\text{MeOD}-d_4$ (δ in ppm).

No.	2	
	δ_{H} , mult. (J in Hz)	δ_{C}
2	-----	145.10
5	-----	80.92
6	2.34 (3H, s)	27.14
8	-----	171.52
9	2.08 (3H, s)	22.57
10	-----	171.16
11	2.25 (3H, s)	23.78
1'	-----	144.70
2'	7.41 (1H, dd, $J=7.5$; 1.5 Hz)	125.92
3'	7.34 (1H, t, $J=7.5$ Hz)	129.53
4'	7.26 (1H, tt, $J=7.5$; 1.5 Hz)	128.75
5'	7.34 (1H, t, $J=7.5$ Hz)	129.53
6'	7.41 (1H, dd, $J=7.5$; 1.5 Hz)	125.92

Table 3. Cytotoxic effects of compounds 1-2.

Compounds	CC ₅₀ ^a (μM)			
	A549	Caki-1	T24	PC-3
Untreated cells	95.94±0.30	92.31±0.49	98.58±0.51	95.86±0.45
CTK8F1368 ^b	0.22±0.35	0.23±0.42	0.23±0.83	0.24±0.20
1	31.07±0.87	28.01±0.52	27.45±0.80	29.72±0.22
2	1.37±0.09	1.35±0.19	1.33±0.88	1.26±0.57

^a The concentration that inhibits 50% of cell growth was calculated (CC₅₀). Data are means of three experiments.

^b Dimethylenastron (CTK8F1368), an anticancer agent, was used as the reference compound.

DATA IN BRIEF

Alkaloids isolated from *Tropaeolum tuberosum* with cytotoxic activity and apoptotic capacity in tumour cell lines

Luis Apaza Ticona^{a,b,*}, Julia Arnanz Sebastián^a, Andreea Madalina Serban^c, Ángel Rumbero Sánchez^a

Affiliation

^a*Department of Organic Chemistry, Faculty of Sciences, University Autónoma of Madrid. Cantoblanco, 28049 Madrid, Spain*

^b*Department of Pharmacology, Pharmacognosy and Botany, Faculty of Pharmacy, University Complutense of Madrid. Ciudad Universitaria s/n, 28040 Madrid, Spain*

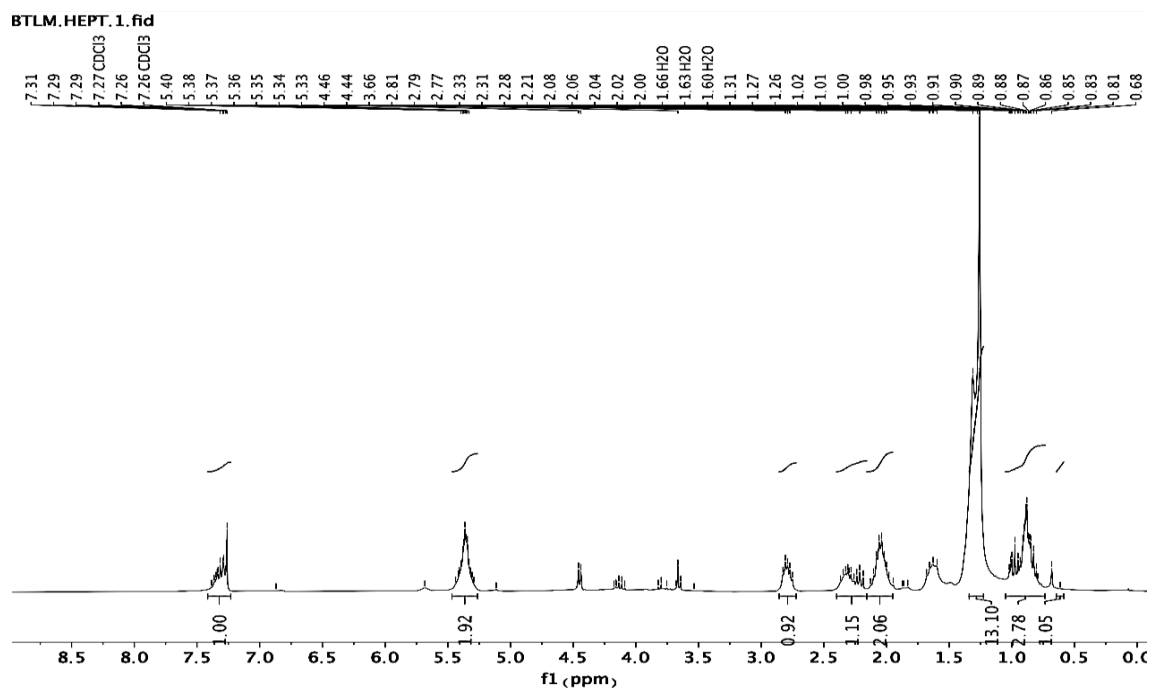
^c*Maria Sklodowska Curie University Hospital for Children. Constantin Brancoveanu Boulevard, 077120 Bucharest, Romania*

*Corresponding author

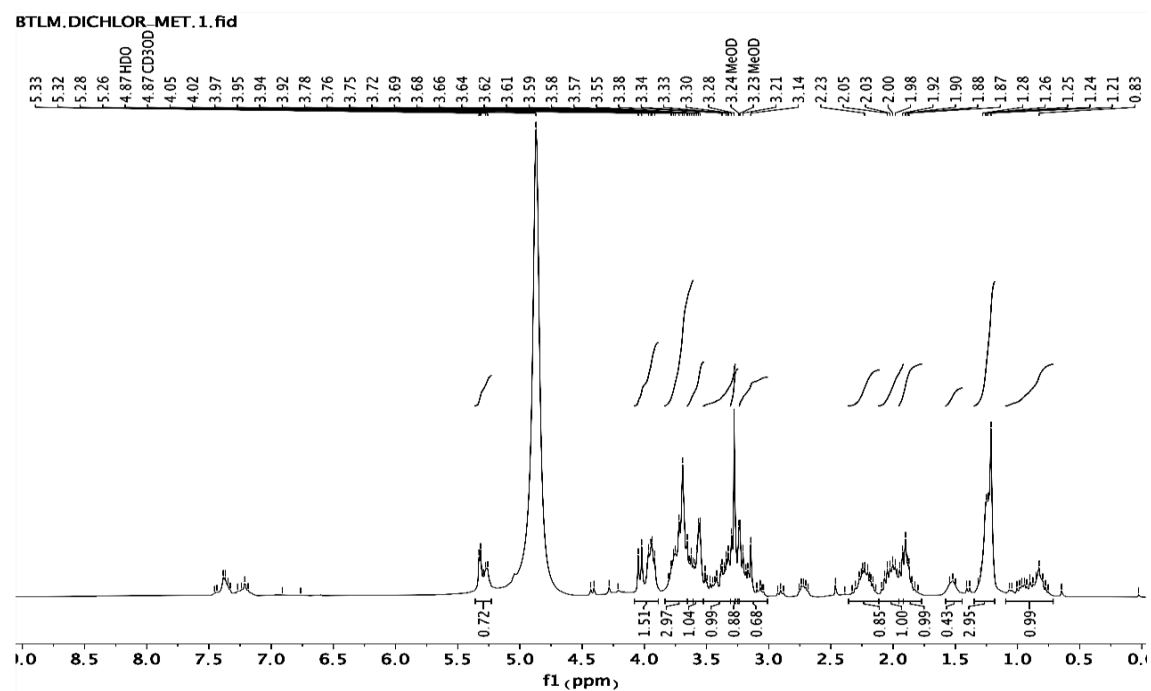
E-mail addresses: luis.apaza@uam.es; lnapaza@ucm.es (Luis Apaza T.).

Table of contents:

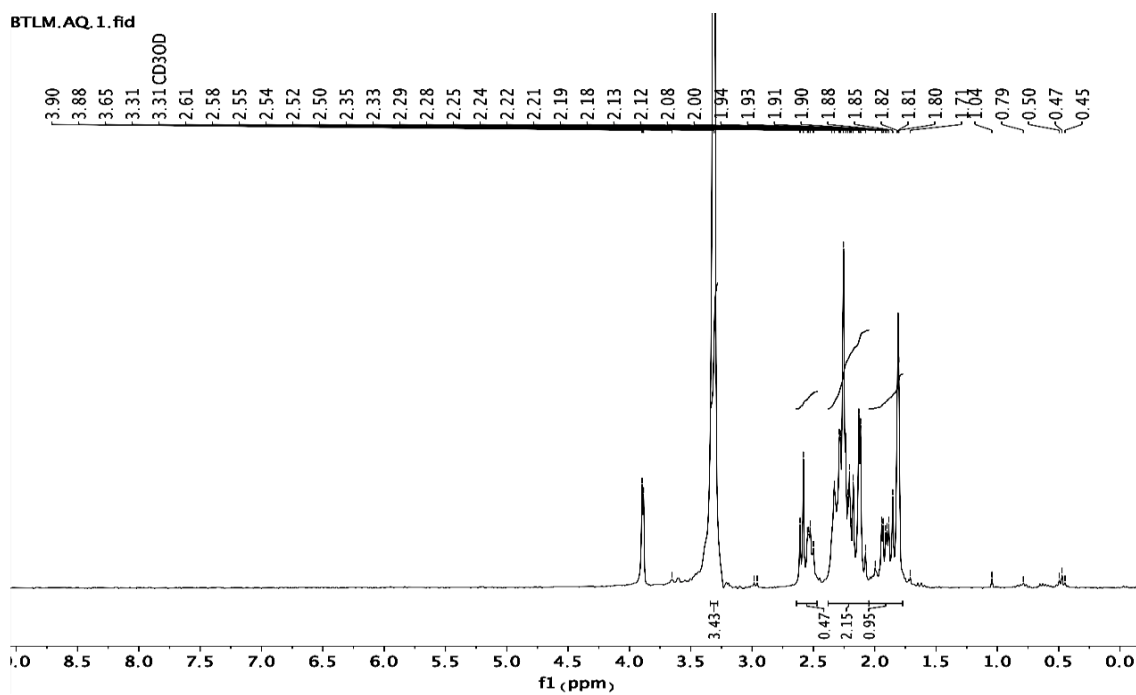
- Figure S1. ^1H -NMR spectrum of n-heptane extract of black tubers from *T. tuberosum* in CDCl_3 300 MHz
- Figure S2. ^1H -NMR spectrum of $\text{CH}_2\text{Cl}_2/\text{MeOH}$ extract of black tubers from *T. tuberosum* in CD_3OD 300 MHz
- Figure S3. ^1H -NMR spectrum of aqueous extract of black tubers from *T. tuberosum* in CD_3OD 300 MHz
- Figure S4. ^1H -NMR spectrum of compound **1** in CDCl_3 250 MHz
- Figure S5. ^{13}C -NMR spectrum of compound **1** in CDCl_3 60 MHz
- Figure S6. DEPT-135 spectrum of compound **1** in CDCl_3 60 MHz
- Figure S7. ^1H - ^1H COSY spectrum of compound **1** in CDCl_3
- Figure S8. HMQC spectrum of compound **1** in CDCl_3
- Figure S9. HMBC spectrum of compound **1** in CDCl_3
- Figure S10. ESI MS spectrum of compound **1**
- Figure S11. ^1H -NMR spectrum of compound **2** in CD_3OD 700 MHz
- Figure S12. ^{13}C -NMR spectrum of compound **2** in CD_3OD 176 MHz
- Figure S13. ^1H - ^1H COSY spectrum of compound **2** in CD_3OD
- Figure S14. HSQC spectrum of compound **2** in CD_3OD
- Figure S15. HMBC spectrum of compound **2** in CD_3OD
- Figure S16. ESI MS spectrum of compound **2**
- Figure S17. Viability of isolated compounds **1** and **2** of black tubers from *T. tuberosum* against a panel of human cell lines, after 72 h of treatment by the XTT assay. Significant diff. among means ($P < 0.0001$)/Tukey's multiple comparisons test



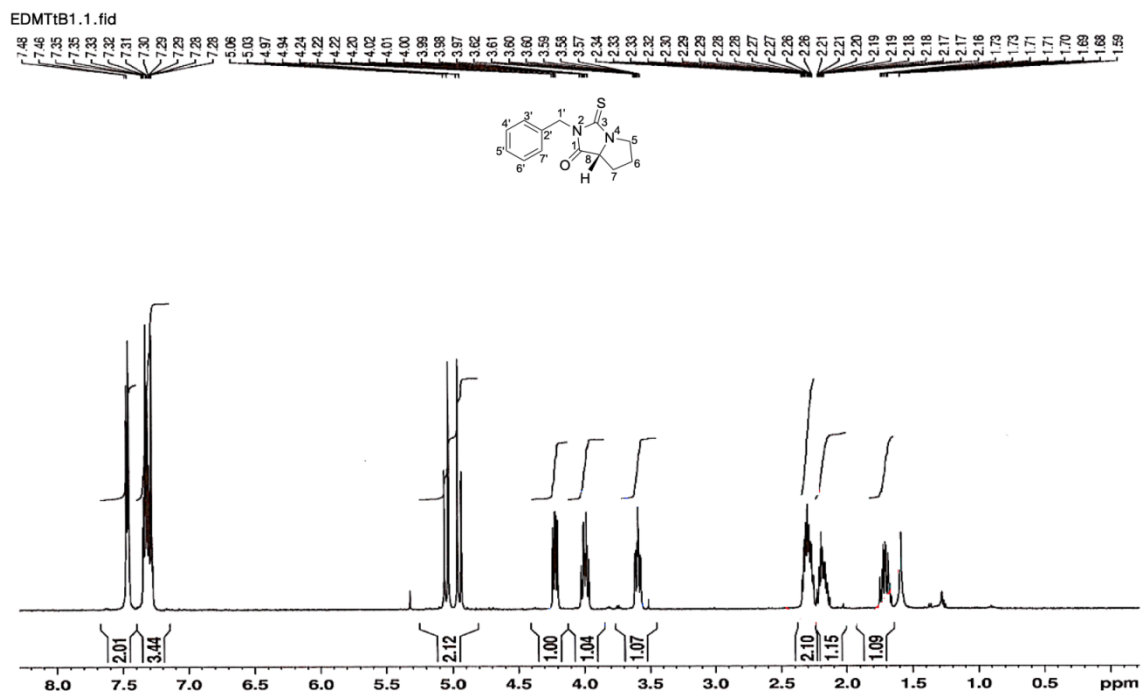
- Figure S1. ¹H-NMR spectrum of *n*-heptane extract of black tubers from *T. tuberosum* in CDCl₃ 300 MHz



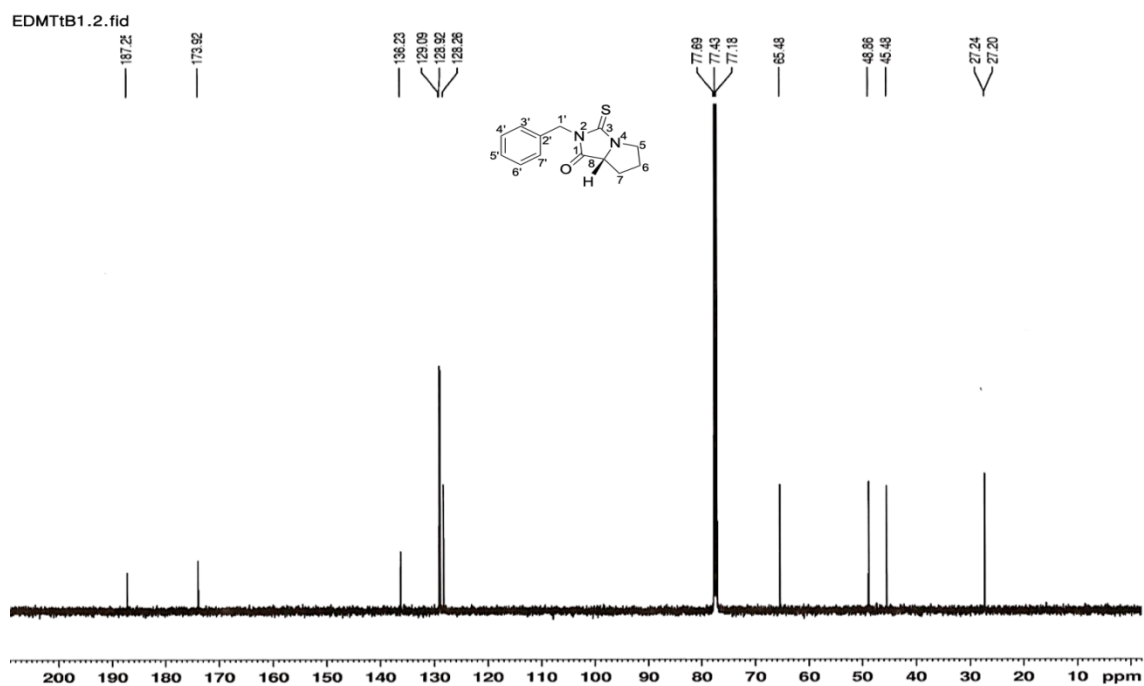
- Figure S2. ¹H-NMR spectrum of CH₂Cl₂/MeOH extract of black tubers from *T. tuberosum* in CD₃OD 300 MHz



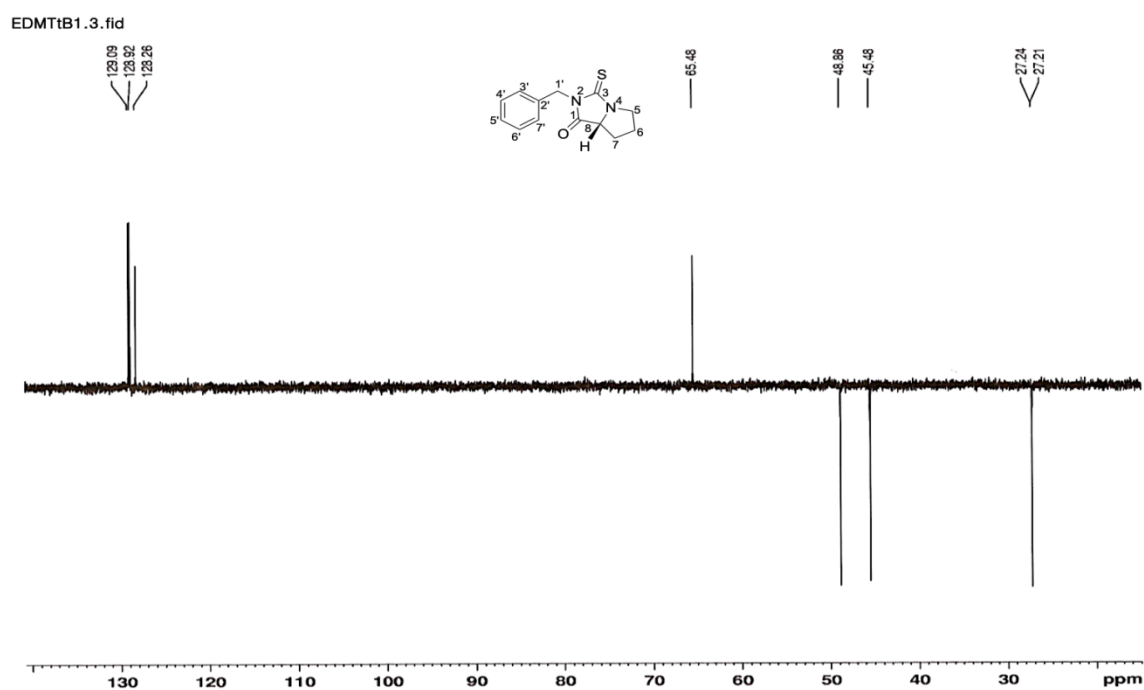
- Figure S3. ^1H -NMR spectrum of aqueous extract of black tubers from *T. tuberosum* in CD_3OD 300 MHz



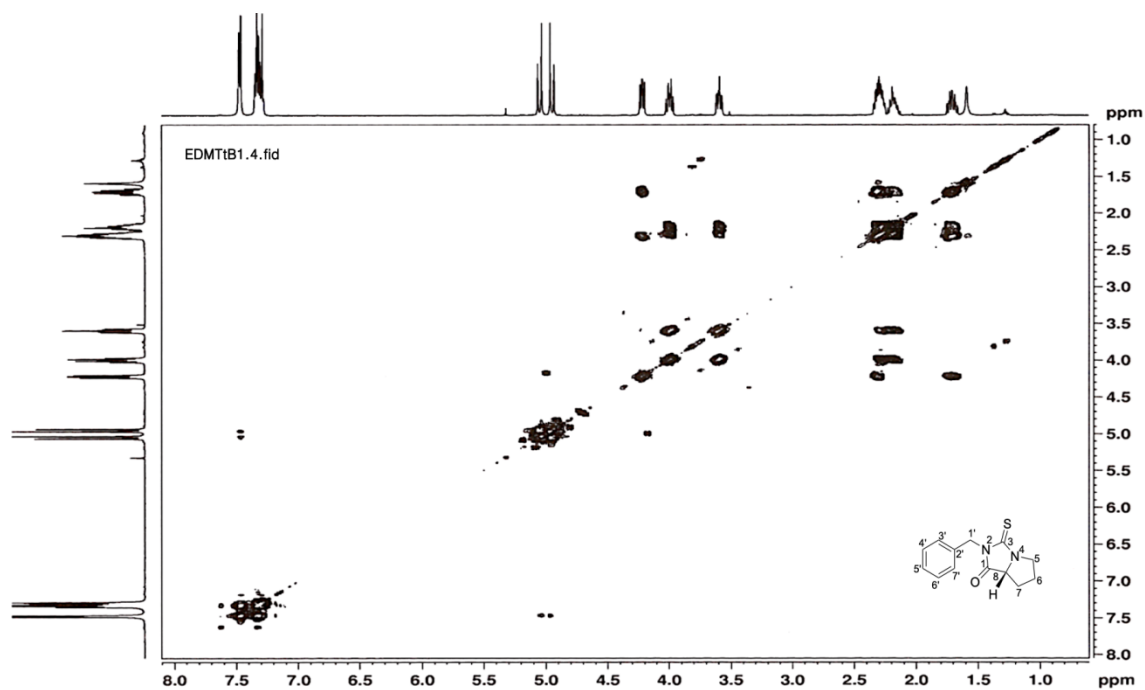
- Figure S4. ^1H -NMR spectrum of compound 1 in CDCl_3 250 MHz



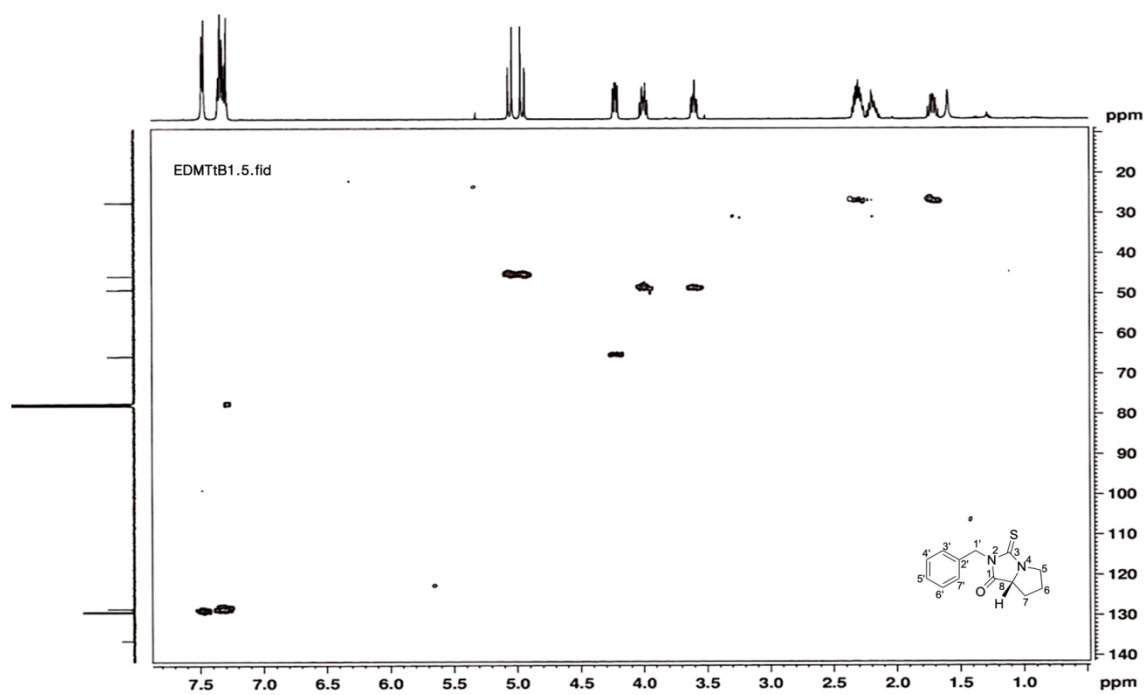
- Figure S5. ^{13}C -NMR spectrum of compound **1** in CDCl_3 60 MHz



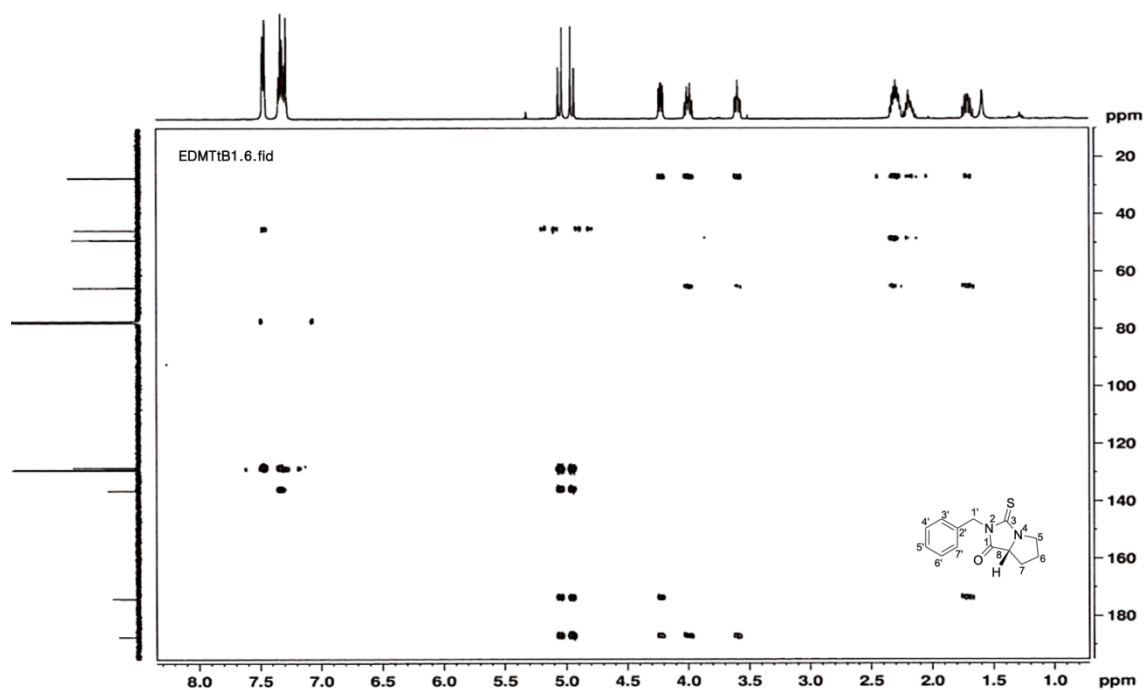
- Figure S6. DEPT-135 spectrum of compound **1** in CDCl_3 60 MHz



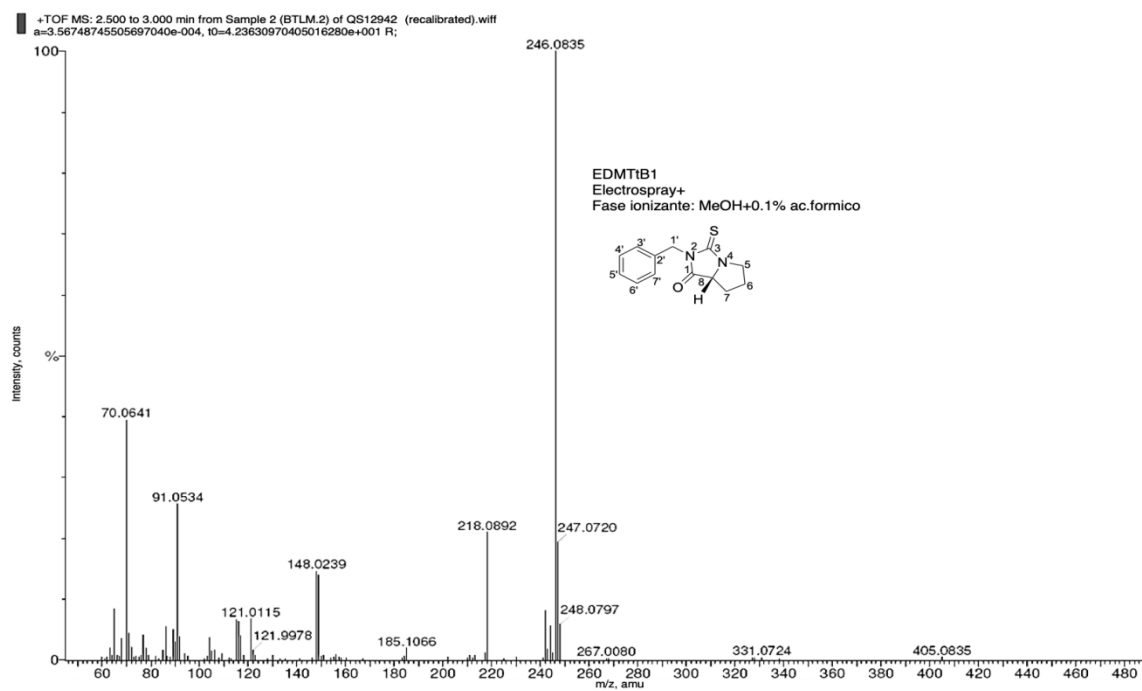
- Figure S7. ^1H - ^1H COSY spectrum of compound **1** in CDCl_3



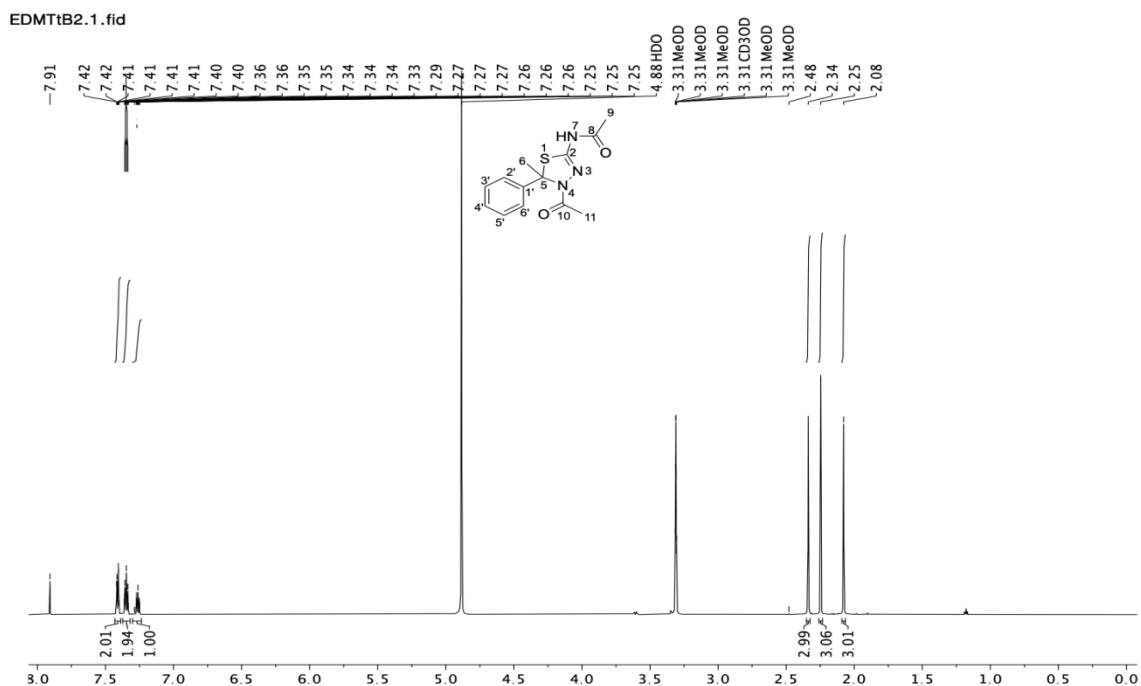
- Figure S8. HMQC spectrum of compound **1** in CDCl_3



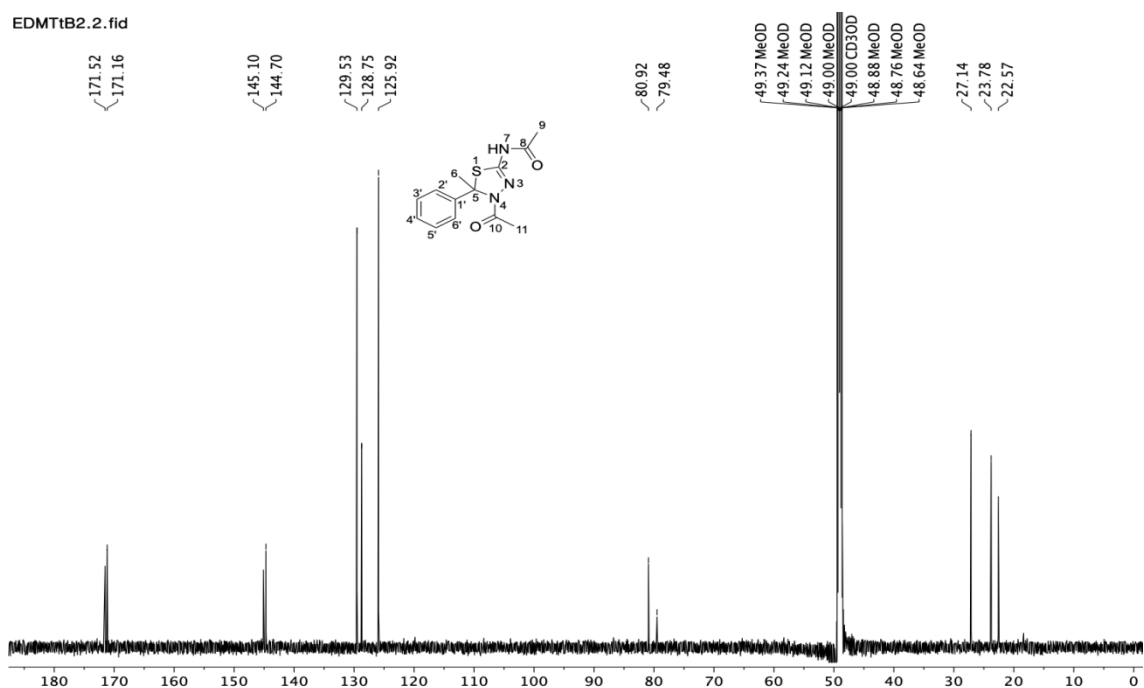
- Figure S9. HMBC spectrum of compound **1** in CDCl_3



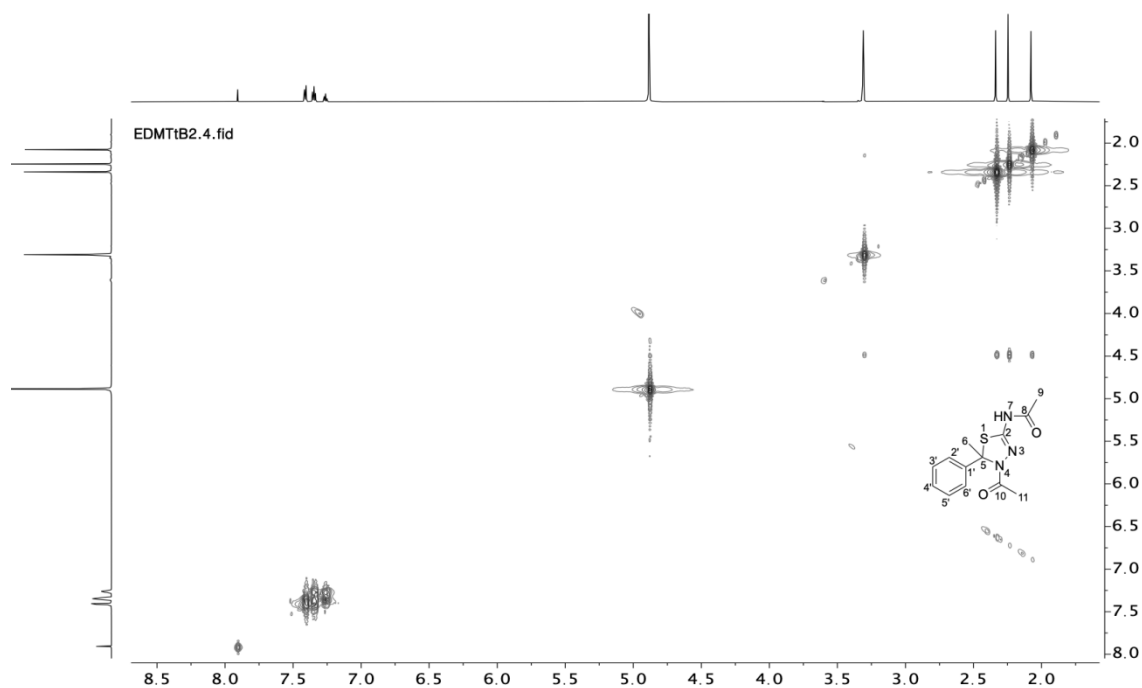
- Figure S10. ESI MS spectrum of compound **1**



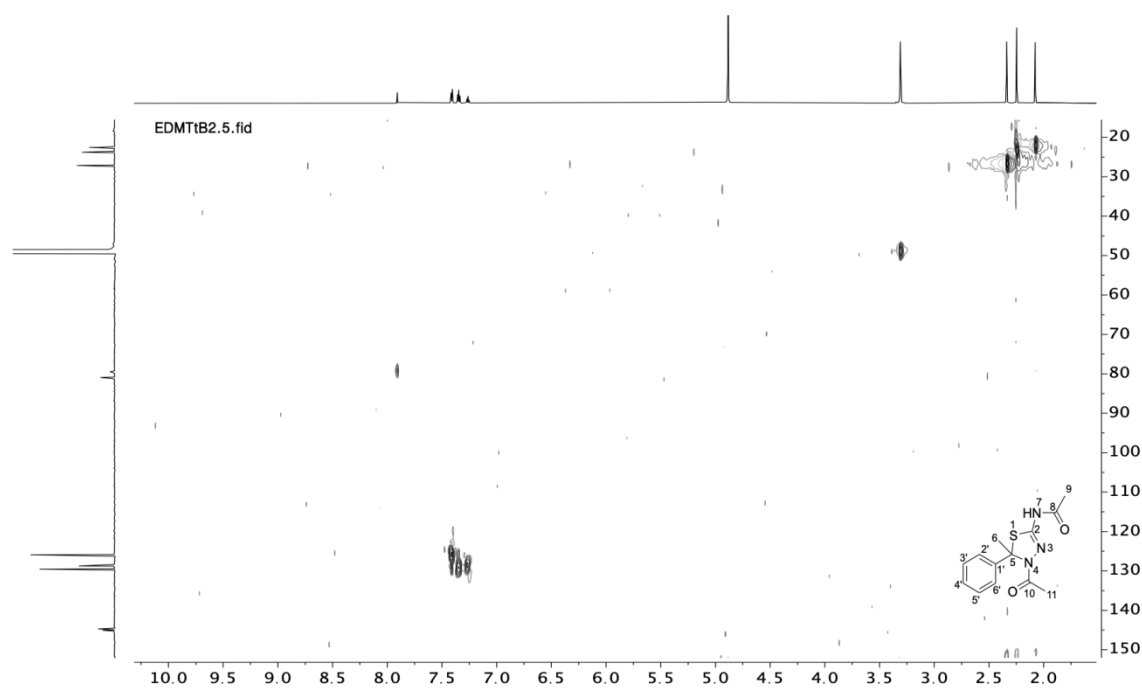
- Figure S11. ^1H -NMR spectrum of compound **2** in CD_3OD 700 MHz



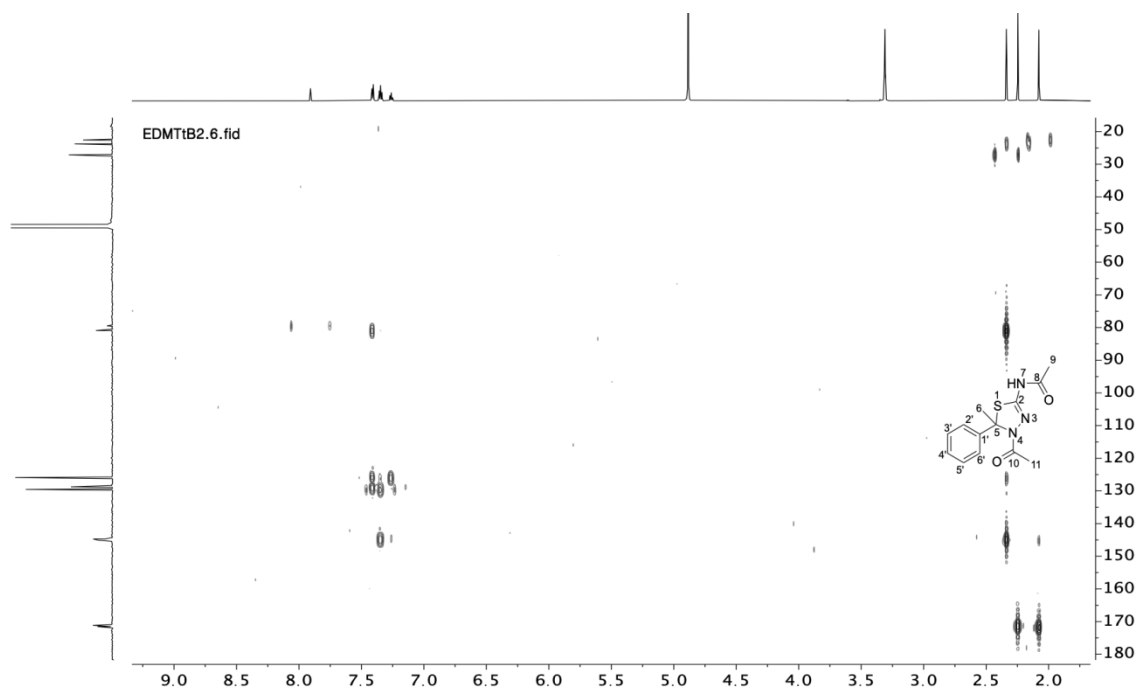
- Figure S12. ^{13}C -NMR spectrum of compound **2** in CD_3OD 176 MHz



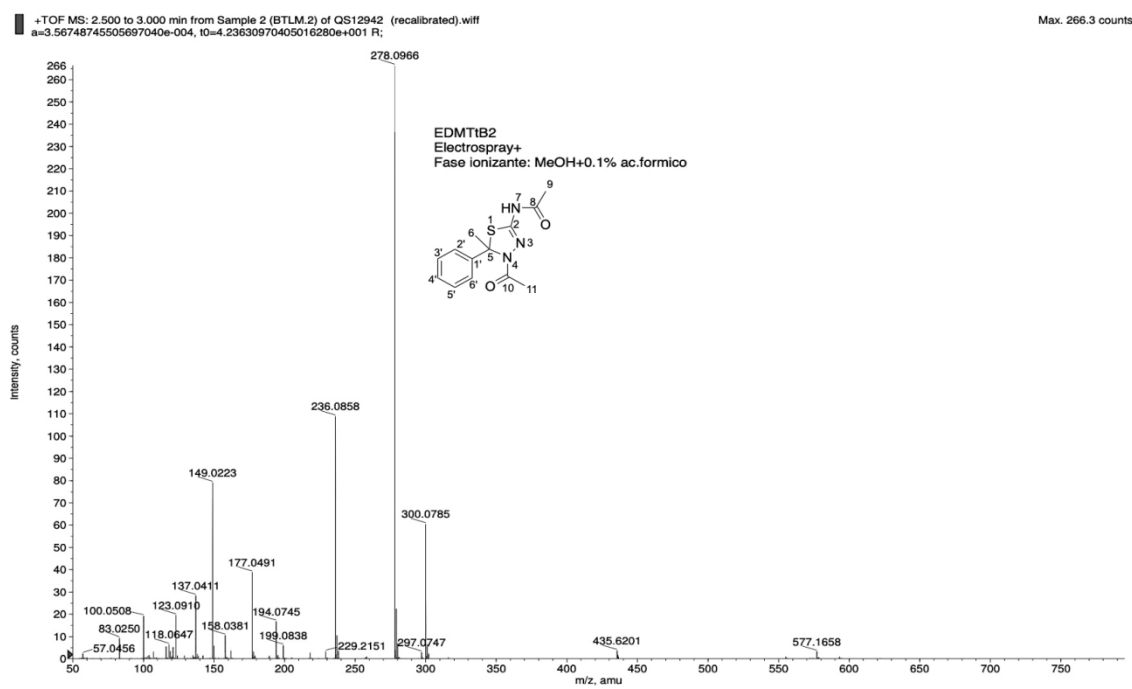
- Figure S13. ^1H - ^1H COSY spectrum of compound **2** in CD_3OD



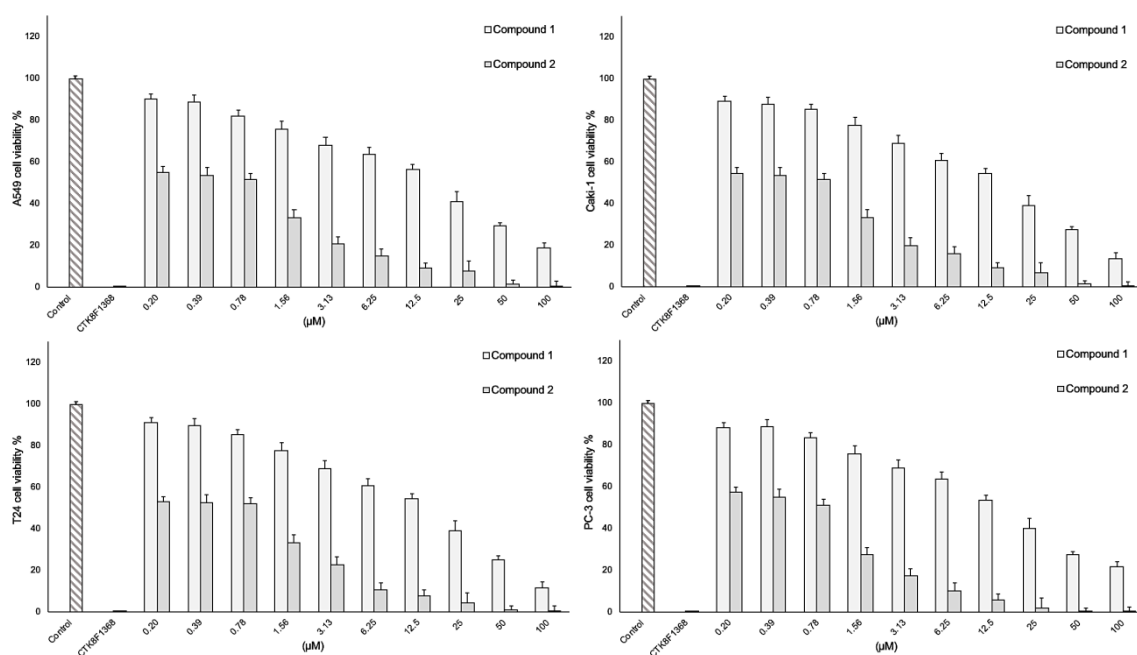
- Figure S14. HSQC spectrum of compound **2** in CD_3OD



- Figure S15. HMBC spectrum of compound **2** in CD₃OD



- Figure S16. ESI MS spectrum of compound **2**



- Figure S17. Viability of isolated compounds **1** and **2** of black tubers from *T. tuberosum* against a panel of human cell lines, after 72 h of treatment by the XTT assay. Significant diff. among means ($P < 0.0001$)/Tukey's multiple comparisons test